CHEMISTRY OF MATERIALS

Open Access

pubs.acs.org/cm

Article

In Situ X-ray Diffraction Study of MXene Synthesis by the Reaction of Ti_3AlC_2 with Molten Zinc and Tin Chlorides

Artem Iakunkov, Nicolas Boulanger, Bartosz Gurzeda, Gui Li, Christoph Hennig, Volodymyr Svitlyk, Mads Ry Vogel Jørgensen, Innokenty Kantor, Igor A. Baburin, Mahiar Max Hamedi, and Alexandr V. Talyzin*

Cite This: Chem. Mater. 2025, 37, 1132–1142

Read Online

ABSTRACT: Using molten salts for etching aluminum (Al) away from the MAX phase for MXene synthesis is an attractive alternative method that allows one to avoid the use of toxic hydrofluoric acid (HF) solutions. However, the mechanism of the MAX phase reaction with molten salts remains to date unclear due to the lack of in situ data. Here, we present a detailed in situ time-resolved synchrotron radiation X-ray diffraction study of the MAX phase annealing in molten $ZnCl_2$ and $SnCl_2$. The reaction of salts with the MAX phase is found to occur in two stages. The initial period of annealing results in the delamination of two-dimensional (2D) Ti_3C_2 layers, vigorous evolution of $AlCl_3$ bubbles, and dissolution of Zn in a $ZnCl_2$ melt. The chlorine-terminated Ti_3C_2 sheets formed in the delaminated state are restacked into a relatively well-ordered MXene structure ($P6_3/mmc$, a = 3.071 Å and c = 18.577 Å) during the prolonged annealing in molten salts. Surprisingly, the data recorded directly in molten salts at temperatures up to 873 K demonstrate that $Ti_3C_2Cl_x$ MXene shows no swelling in both liquid $ZnCl_2$ and $SnCl_2$. The structure of MXene studied directly in the molten salts is found to be the same as in ex situ experiments performed after cooling and water washing under ambient conditions. The absence of the "pristine" melt-swollen phase indicates a rather different mechanism of MXene formation compared to HF-based solution methods. Formation of MXene by gradually removing Al from the MAX phase starting at the edges of flakes and propagating into the deeper parts of interlayers is not possible, since the molten salt is not capable of penetrating between Cl-terminated Ti_3C_2 layers.

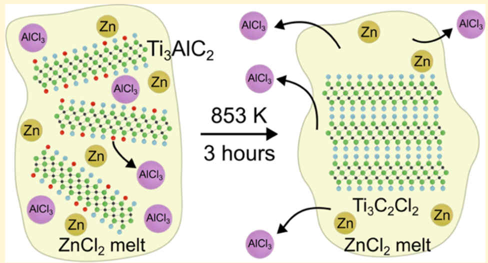

■ INTRODUCTION

MXenes are materials composed of two-dimensional (2D) sheets of transition metal carbides.[1,2] Strong interest in MXenes over the past decade has been motivated by the broad range of proposed applications, including energy storage,[3,4] water purification,[5] electromagnetic interference shielding,[6] biomedical applications,[7] wear-resistant coatings,[8] and electronics.[9]

MXenes are synthesized by selectively etching "A" layers of metal atoms from their layered precursors (MAX phases) while retaining the MX layers with a two-dimensional structure.[2] The most studied MXene so far is $Ti_3C_2T_X$ produced by etching aluminum (Al) away from the Ti_3AlC_2 structure.[10,11] $Ti_3C_2T_x$ can be delaminated to produce true 2D sheets by dispersing it in suitable polar solvents, e.g., dimethyl sulfoxide (DMSO).[11,12] The 2D Ti_3C_2 sheets comprising Ti-MXene are terminated by several kinds of functional groups, including fluorine, oxygen, and hydroxyls, denoted "T_x", but the exact type of termination is still somewhat uncertain and depends on synthesis procedures.[13,14]

The most common MXene synthesis route is wet chemical etching using hydrofluoric acid (HF)[10] and, more recently, the use of strong acids together with Li salts such as "HF + LiCl"[13,15] or "LiF + HCl".[16] In the latter case, the etching agent is again HF. Our recent in situ X-ray diffraction (XRD) experiments demonstrated that "pristine" MXene studied prior to water washing has a structure intercalated with one layer of HF solution.[17] The etching of Al is then limited to one-layer thickness "channels" provided by the replacement of Al with HF molecules. Conventional MXene is produced by water washing, which needs to be considered as the last step of chemical synthesis. The reaction of pristine MXene with water removes HF intercalated between MXene layers, possibly also adding some oxygen groups to the surface of MXene sheets.[17]

Using toxic HF for the synthesis of MXenes is environmentally undesirable and is a serious hindrance to mass production. Therefore, alternative methods not involving HF for the synthesis of MXenes are of great importance for the wider implementation of these materials in realistic applications.

Received: October 28, 2024
Revised: January 10, 2025
Accepted: January 13, 2025
Published: January 21, 2025

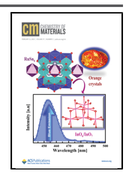

https://doi.org/10.1021/acs.chemmater.4c02989
Chem. Mater. 2025, 37, 1132–1142

One of the most attractive alternatives to HF synthesis routes developed very recently is based on etching performed in molten salts serving as a Lewis acid.[18−20] The Lewis Acid Molten Salt Etching (LAMS) is fluoride-free but requires using relatively high temperatures for etching the Al layer from the MAX phase.[18] Zinc, tin, copper, and some other metal chlorides have been successfully used as Lewis acids for the preparation of $Ti_3C_2T_x$.[20−24]

Unlike the MXene sheets prepared using wet chemical methods, which are believed to be terminated (at least partly) by fluorine- and oxygen-containing functional groups, using molten chloride salts suggests that MXene sheets prepared by the LAMS method must be terminated by chlorine.[20,24,25] The experimental report supported by theoretical simulations suggests the composition of molten salt MXene as $Ti_3C_2Cl_2$.[25]

Therefore, it is expected that some properties of MXenes prepared by these routes (e.g., stability in water) can be significantly different. In particular, several studies report that $Ti_3C_2Cl_x$ prepared by the LAMS method is difficult to disperse in aqueous solutions.[26,27] Therefore, modification of the surface chemistry of MXenes prepared by the LAMS method is also rather actively expanding the research field.[28,29]

The exact mechanism of MXene synthesis by the reaction with molten salts is also still under debate. It is suggested that the etching of Al from the MAX phase occurs by the reaction with, e.g., molten $ZnCl_2$ and the formation of gaseous $AlCl_3$ and metallic Zn. The Ti_3C_2 layers formed after the removal of Al are terminated by chlorine, forming $Ti_3C_2Cl_x$.[20] A relatively large excess of molten salt (mole ratio 6:1) is required for successful MXene synthesis from the MAX phase using the LAMS method. The existence of Zn-substituted MAX phase Ti_3ZnC_2 was also reported for experiments with a relatively small amount of molten $ZnCl_2$ added to the MAX phase (mole ratio of 1.5:1).[20] However, the formation of the Ti_3ZnC_2 phase is completely avoided in experiments with a large excess of molten salt.[26]

It is important to note that most studies of MXenes produced by the LAMS method are limited to ex situ analysis of materials after cooling the reaction mixture and extensive washing to eliminate other reaction products.[18] High temperatures of LAMS synthesis (600−750 °C) and the need to record data in liquid molten salts complicate in situ studies of the reaction mechanism, making it the perfect subject for synchrotron radiation XRD studies.

Only one in situ structural study of MXene synthesis by the LAMS method is so far available. This study reports XRD data for a relatively exotic Nb-MAX phase synthesized using the Nb_2GaC precursor.[30] Surprisingly, so far, no in situ studies are available for the synthesis of the most common $Ti_3C_2T_x$ MXene phase using the Ti_3AlC_2 MAX phase as a precursor. Considering that −OH-terminated Ti-MXene shows easy swelling in water[31] and aqueous HF solution,[17] we anticipated that Cl-terminated Ti-MXene would be exhibiting swelling in molten chloride salts. Surprisingly, this suggestion was not confirmed.

Here, we report the in situ synchrotron radiation XRD study of $Ti_3C_2Cl_x$ synthesis by the reaction of the Ti_3AlC_2 MAX phase with molten $ZnCl_2$ and $SnCl_2$ at elevated temperature conditions. Complete transformation of the MAX phase into MXene was achieved in molten $ZnCl_2$, and a detailed analysis of the sample materials as a function of annealing time is presented. The reaction proceeds with the formation of delaminated Ti_3C_2 layers at the initial stage of annealing. It is suggested that the removal of Al from the MAX structure, the termination of 2D titanium carbide layers with chlorine, and formation of elemental Zn dissolved in $ZnCl_2$ occur in the delaminated phase, which is an intermediate between MAX and MXene. The $Ti_3C_2Cl_x$ phase is found to form after prolonged annealing suggestively by restacking 2D layers of chlorine-terminated Ti_3C_2 formed initially in the delaminated phase. The MXene formed in the molten salts (both $ZnCl_2$ and $SnCl_2$) has the same structure and shows no swelling in the molten salts. The surprising absence of melt-swollen "pristine MXene" indicates a reaction mechanism that is rather different compared to HF-based aqueous solution methods.

■ EXPERIMENTAL SECTION

Materials and Synthesis. $ZnCl_2$ and $SnCl_2$ (reagent grade, 98%) were purchased from Sigma-Aldrich and used without additional purification. MAX phase Ti_3AlC_2 precursor was purchased from Carbon-Ukraine.

For the synthesis of bulk samples, a powder mixture of Ti_3AlC_2 and $ZnCl_2$ in a 1:6 molar ratio was loaded into ∼7 mm diameter borosilicate glass tubes under nitrogen, and the tubes were sealed under dynamic vacuum (∼10^{-5} bar). The tubes with the sample were then heated in a standard tubular furnace with a rate of 8 K/min up to 853 K. After annealing at 853 K (1 min for one sample and 3 h for the other), the samples were cooled by switching off the furnace to achieve the maximal cooling rate. The samples were washed with water and characterized by XRD using an in-house Panalytical X'pert X-ray diffractometer with Cu Kα radiation (λ = 1.5406 Å).

In Situ Synchrotron Characterization. An in situ synchrotron radiation X-ray diffraction study was performed using MAX phase and chloride salt powders premixed in agate mortar in different molar proportions inside a nitrogen-filled glovebox (to avoid salt hydration by air moisture) and loaded into Hilgenberg special glass capillaries. Capillaries were loaded with the powder mixture only for about 1/3 of the length to keep some space for evolving gases and for the condensation of reaction products in the cold zone. Material-filled capillaries were taken out of the glovebox and briefly exposed to air for torch sealing.

The samples were heated inside sealed capillaries typically up to 853−873 K, kept at this temperature for several hours, and cooled down. 2D XRD images were continuously recorded during the whole heating/cooling cycle during several hours lasting experiments. Heating guns with somewhat different hotspot sizes were used in experiments performed at ESRF and at MAX IV synchrotron facilities; in both cases, the size of the cold zone was larger than the size of the hot zone. In this case, gaseous reaction products are mostly removed into an empty cold zone due to the process of reaction condensing on the walls of the capillary.

In situ synchrotron characterization of MXene synthesis was conducted at the Rossendorf Beamline (BM20) of the European Synchrotron Radiation Facility (ESRF)[9] using a radiation wavelength (λ) of 0.7381 Å. A hot air gas blower (FMB Oxford DGB-1) was used for the annealing experiments. Experimental data were collected in transmission geometry using a DECTRIS PILATUS3 X 2M detector and analyzed with Bubble software.[32] The detector geometry parameters were calibrated using the NIST (SRM660x) LaB_6 standard with PyFAI software. The samples were heated typically up to 823−873 K with a heating rate of 2−5 K/min, and 60 s scans were recorded continuously.

The second part of the experiments was conducted at the DanMAX beamline at the MAX IV Laboratory. The temperature was controlled by using a HyBec Hi-Heater controlled by a Lakeshore 336 temperature controller. The diffraction data were collected up to a maximum 2θ of 28° (Q_{max} ∼ 3.75 Å^{-1}) using a wavelength of 0.8266 Å (15.00 keV) on a DECTRIS PILATUS3 X 2M CdTe area detector. The wavelength and geometry of the instrument were refined using a LaB_6 standard (NIST SRM660c) and the program PyFAI.[33] The raw area detector data were azimuthally integrated to intensity versus 2θ

https://doi.org/10.1021/acs.chemmater.4c02989
Chem. Mater. 2025, 37, 1132−1142

using the MatFRAIA algorithm.[34] The maximum temperature studied in these experiments was 823 K, with a heating rate of 5 K/min, and each scan lasted for 1 s.

The $Ti_3C_2Cl_2$ structure model was built by rescaling the known Ti_3C_2 structure to the experimentally determined unit cell and terminating the coordination spheres of Ti atoms with Cl. Atomic coordinates were not refined against XRD data, since a meaningful Rietveld refinement is not possible for given data quality (too few reflections and multiphase sample).

■ RESULTS

The main objective of this work was to study in situ the reaction of MAX phase etching in molten salts, leading to formation of MXenes. These experiments aimed to reveal the structure of pristine MXene still immersed in molten salts. The structure of Ti-MXene prepared by the LAMS method was so far reported only after cooling and water washing.[24,27,35] Structural analysis of phases evolving in the process of MAX phase etching and MXene formation was performed by using synchrotron radiation XRD data for the two systems. Etching of the MAX phase in molten $ZnCl_2$ is presented first, followed by results obtained for $SnCl_2$ etching.

Reaction of the MAX Phase with Molten $ZnCl_2$. An in situ synchrotron radiation X-ray diffraction study was performed using Ti_3AlC_2 MAX phase and $ZnCl_2$ powders premixed in different molar ratios, loaded into sealed glass capillaries, and heated above the melting point of the salt for periods up to 6 h. The best results were obtained for the sample premixed in a 1:6 molar ratio of $Ti_3AlC_2/ZnCl_2$ in agreement with earlier ex situ studies.[18,20]

The reference XRD pattern recorded from Ti_3AlC_2 powder showed the high purity of the precursor material with unit cell parameters refined using 21 reflections in the $P6_3/mmc$ space group (a = 3.071 Å and c = 18.577 Å) in good agreement with literature data.[10,20] Experimental and theoretically simulated patterns of Ti_3AlC_2 are compared in Figure S2 in the SI file.

XRD patterns recorded from a mixture of Ti_3AlC_2 and $ZnCl_2$ powders (mixed in a 1:6 molar proportion) are dominated by a large number of very strong reflections from $ZnCl_2$ (Figures 1 and S2 in the SI file). The mixed $Ti_3AlC_2/ZnCl_2$ sample was rapidly heated to 853 K and kept at this temperature for ∼280 min, while 2D XRD images were continuously recorded every 60 s, thus providing detailed time-resolved characterization of phases formed in the process of the Ti_3AlC_2 reaction with molten $ZnCl_2$.

Above the melting point, all reflections from crystalline $ZnCl_2$ disappeared (Figures S2 and S3), and a new broad feature from the liquid salt appeared (Figure S2 in the SI file). The XRD pattern recorded just above the melting point of salt at 590 K (Figure S3) still shows only reflections of the precursor Ti_3AlC_2 with unit cell parameters a = 3.083 Å and c = 18.635 Å, which are only slightly higher than those at ambient temperature due to thermal expansion.

Further heating of the MAX phase in molten $ZnCl_2$ resulted in dramatic changes in the sample appearance and structure. Intensive bubbling was observed in the heating zone of the capillary above the melting point of $ZnCl_2$ as the temperature approached 853 K, correlating with a significant drop in the intensity of all XRD reflections (Figure 1).

The strongest reflections of the MAX phase were still observed at the moment of intense bubbling but dropped in intensity rather significantly. This bubbling obviously disturbs data recording due to the movement of the powder and liquid enclosed in the capillary. However, as will be discussed below,

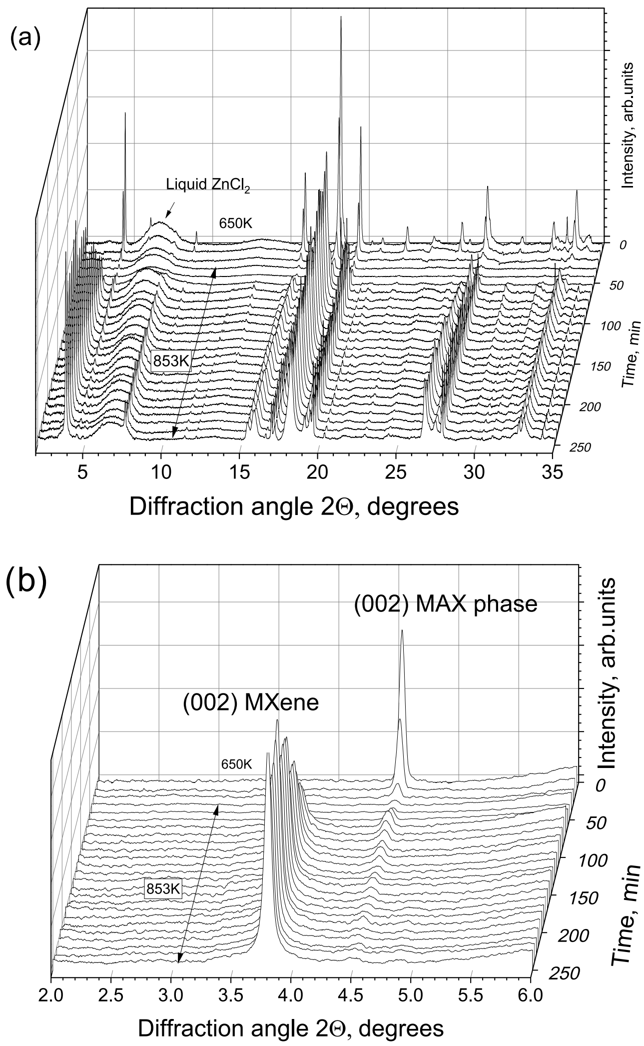

Figure 1. (a) Selected XRD patterns recorded from the sample of $ZnCl_2$ and Ti_3AlC_2 premixed in a 6:1 mole ratio and annealed at 853 K (λ = 0.73804 Å). Every 10th pattern is shown focusing on the temperature region of liquid $ZnCl_2$ (see Figures S2 and S3 in the SI file for the data recorded just below and above the temperature point of $ZnCl_2$ melting during heating). (b) Low-angle part of XRD patterns showing (002) reflections of precursor Ti_3AlC_2 and MXene formed by the reaction with $ZnCl_2$. Some background was subtracted from all patterns.

this initial stage of the reaction also results in a true loss of MAX phase structure ordering. The bubble formation slowed down after about 20 min of annealing at 853 K, and a new set of reflections emerged (Figure 1a).

The formation of MXene at this moment is clearly evidenced by the appearance of the (002) reflection with a d-spacing of 11.1 Å (Figure 1b). The etching reaction can be easiest followed by observing the increase in the intensity of the broader (002) reflection from the MXene (d = 11.1 Å) over the time of the reaction, while the intensity of the relatively sharp (002) reflection from the precursor MAX phase (∼9.4 Å) fades (Figures 1b and 2c).

The intensity of the (002) reflection of the MAX phase faded sharply at the initial stage of the reaction and disappeared nearly completely after ∼3 h of annealing in $ZnCl_2$ at 853 K (Figures 1 and 2a). The d(002) value of the MAX phase increased linearly due to the thermal expansion at

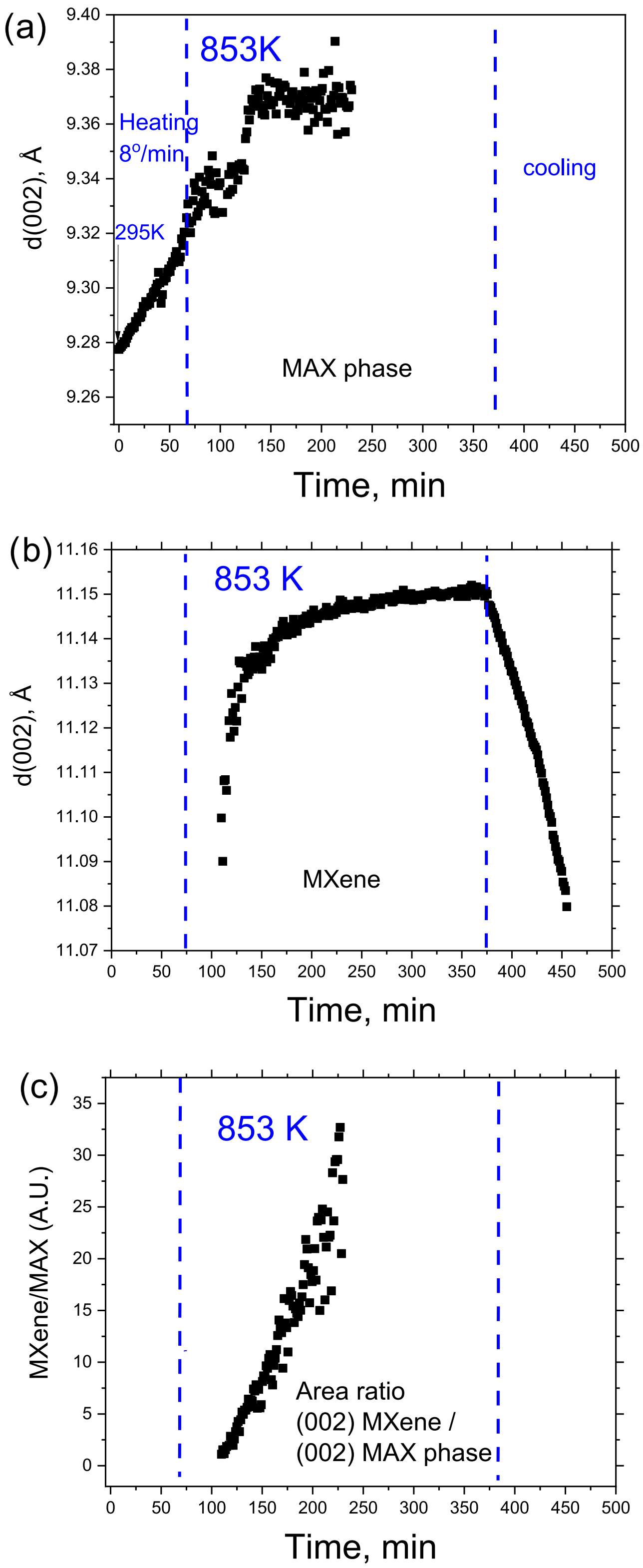

Figure 2. Time evolution of $d(002)$ for the precursor MAX phase (a) and $d(002)$ for MXene (b) recorded during the annealing experiment performed for sample premixed in a 1:6 proportion of $Ti_3AlC_2/ZnCl_2$. The area ratio for (002) reflections of the MXene/MAX phase (c).

temperatures below the melting point of $ZnCl_2$, but it also continued to increase slightly (by ∼0.04 Å) for about 1 h at 853 K (Figure 2a). The slight expansion of the MAX phase structure correlates with a very strong drop in the intensity of the (002) reflection and intense bubble formation inside the capillary observed visually. It is important to note that the remaining traces of the crystalline MAX phase still correspond to Ti_3AlC_2 rather than Zn-substituted Ti_3ZnC_2 (Figure S3 in the SI file).

The MXene (002) reflection first appears after the end of the intense bubbling period (time region from 100 to ∼225 min in Figure 2c). The $d(002)$ value of MXene slightly increases in the initial stage of annealing but remains almost unchanged at ∼11.15 Å over the next 3 h. The intensity of the (002) reflection increases during the first 3 h of annealing and remains nearly the same after longer annealing, indicating complete MAX phase conversion into MXene (Figure 2b). The integral peak intensity ratio of MXene(002)/MAX(002) reflections showed a linear increase during annealing at 853 K (Figure 2c).

A detailed analysis of the XRD pattern recorded at the end of the heating is shown in Figure 3. The analysis of this pattern shows that all major reflections are not from the precursor MAX phase and can be assigned to the newly formed MXene

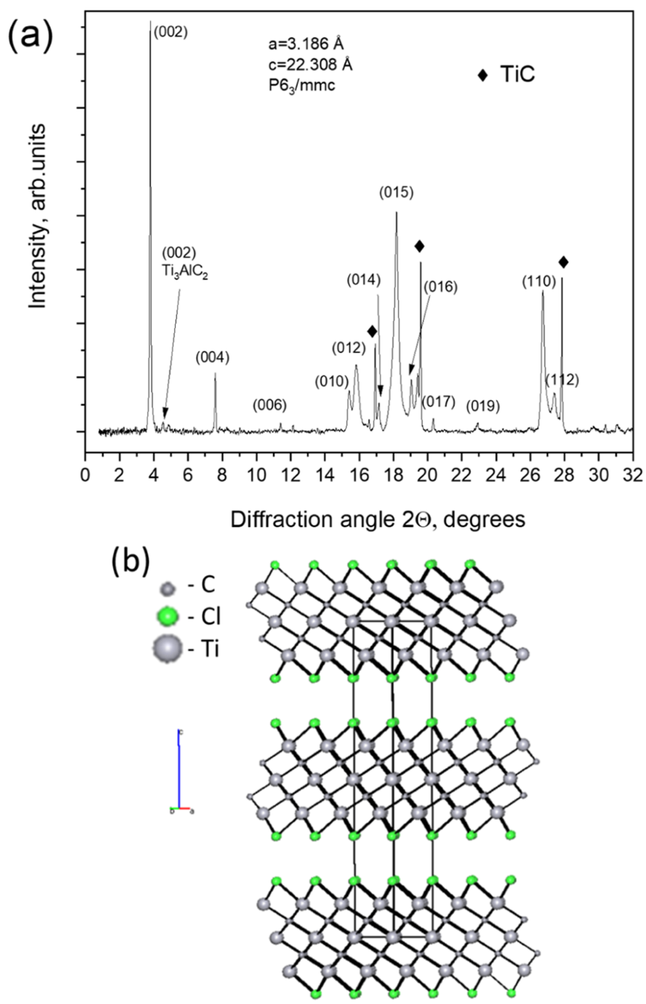

Figure 3. (a) XRD pattern recorded directly in molten salt after ∼215 min of annealing at 853 K. For this figure, background subtraction also included the feature originating from molten $ZnCl_2$. The samples of the MAX phase and $ZnCl_2$ were premixed in a 1:6 molar ratio in this experiment (see also Figure 1). Radiation wavelength λ = 0.73804 Å. (b) Structure model of $Ti_2C_2Cl_2$ simulated using experimental unit cell parameters.

https://doi.org/10.1021/acs.chemmater.4c02989
Chem. Mater. 2025, 37, 1132−1142

structure. See Figure S3 in the SI file, where the XRD pattern of the MAX phase recorded directly after the melting of the $ZnCl_2$ is plotted together with the XRD pattern recorded at the end of annealing.

Notably, the structure of MXene found in our experiments shows relatively good ordering of 2D titanium carbide layers. This is in strong contrast to the structure of Ti-MXene synthesized using HF-related solution routines, which typically demonstrates the absence or very poor ordering of 2D layers. Typically, XRD patterns of $Ti_3C_2T_x$ prepared using HF etching show a strong 00*l*- set of reflections and rather broad features due to other lattices, most likely due to the presence of a variety of terminating functional groups (T_x) with x corresponding to −F, −OH, and possibly some other groups.[10,11,17,36] That is not the case for $Ti_3C_2Cl_2$, which exhibits about 15 relatively sharp XRD reflections besides the 00*l*- set. The most likely reason for better ordering is the absence of terminating groups other than chlorine. Considering reports of pure Cl termination of LAMS MXene, the ideal composition $Ti_3C_2Cl_2$ of this MXene has been considered in earlier studies.[25] However, experimental materials are likely to deviate from the perfect stoichiometry; thus, it is more relevant to assume $Ti_3C_2Cl_x$ composition.

The set of new strong reflections that appear after the reaction of the MAX phase with molten $ZnCl_2$ is interpreted as MXene $Ti_3C_2Cl_x$ and indexed using unit cell parameters a = 3.186 Å and c = 22.312 Å ($P6_3/mmc$), Figure 3a. Note that the a-parameter of the MXene structure is about 0.1 Å larger compared to the a-parameter of the precursor Ti_3AlC_2. The unit cell parameters calculated for MXene formed in our experiments agree with a structural model of $Ti_3C_2Cl_2$ constructed in our study, assuming complete termination of the 2D layers with chlorine (Figure 3b). A simulated XRD pattern for the $Ti_2C_2Cl_2$ structure shown in Figure 3b shows reasonable agreement with the experimental pattern (Figure S6) considering the multiphase nature of the sample, which also includes TiC and some peaks likely originating from the remaining disordered MAX phase.

The pattern shown in Figure 3 shows only a rather weak (002) reflection from the MAX phase and a relatively strong set of reflections from TiC. The formation of TiC can be explained if some Ti_3C_2 layers formed by etching away Al are not immediately terminated by chlorine instead of forming a $Ti_3C_2Cl_x$ restack into a titanium carbide lattice.

Possibly the most surprising finding of our study is the absence of MXene swelling in molten $ZnCl_2$. Prior to experiments, we anticipated that the structure of $Ti_3C_2Cl_x$ would be found in our experiments in a $ZnCl_2$ melt-swollen state, expanded in the c-direction compared to ambient water-washed and solvent-free MXene. A similar HF-swollen structure of pristine MXene was found in our recent experiments with HCl + LiF synthesis.[17] The interlayer distance of pristine MXene recorded directly in HF solution was found to be expanded by ∼3 Å compared to the standard MXene studied ex situ in a solvent-free state. However, the c-unit cell parameter of $Ti_3C_2Cl_x$ recorded in situ (22.33 Å) at 853 K in a melt-immersed state appeared to be nearly the same as in earlier ex situ (22.24 Å) studies performed with water-washed and solvent-free materials.[20] Essentially the same c-unit cell parameter was found also in our experiments after cooling the sample below the melting point of $ZnCl_2$ (Figure S5 in the SI file) and further cooling down to ambient temperature. Therefore, no pristine MXene is found in molten salt synthesis.

It is also interesting to note the absence of XRD reflections from metallic Zn in all XRD patterns recorded in our in situ experiments (Figure 1). The temperature of annealing is above the melting point of Zn (695.5 K), but no reflections from metallic zinc were observed even after cooling below the melting point and even after $ZnCl_2$ solidification.

The analysis of the data recorded during the transformation of the MAX phase into MXene during annealing in molten $ZnCl_2$ indicates the absence of other crystalline intermediate phases. For example, we do not find clear evidence for the formation of Ti_3ZnC_2, which was earlier found in experiments with small loading of $ZnCl_2$.[20] Figure S3 shows the comparison of theoretical XRD patterns of Ti_3ZnC_2, Ti_3AlC_2, and experimental patterns of the MAX phase recorded during initial stages of etching prior to the appearance of MXene reflections.

However, the strong drop in the intensity of the MAX phase reflections at the initial stages of annealing (∼20 min, Figure 1) can be considered an indication of the appearance of an intermediate phase with a strongly disordered structure.

The very strong drop in the intensity of MAX phase reflections prior to the emergence of MXene could be interpreted in two ways. The most trivial explanation suggests that the changes in intensity observed during the first 10−20 min of annealing are simply a result of bubbling and a related disturbance of data recording. The second explanation suggests a loss of long-range order or nearly complete delamination of Ti_3C_2 layers due to the etching of Al and formation of gaseous $AlCl_3$. In the latter case, the drop in the intensity of MAX phase reflections would also still be observable in ex situ experiments for the sample rapidly cooled after short annealing at 853 K.

Therefore, additional synthesis experiments were performed using bulk powder samples and ex situ XRD characterization to verify the structure of materials formed at the initial stage of the etching reaction. Two samples of a $Ti_3AlC_2/ZnCl_2$ mixture (1:6) were annealed at 853 K for short and long periods of time in sealed tubes to make the conditions of synthesis as close as possible to in situ experiments. The first sample was kept at the maximal temperature of 853 K for only 1 min, thus minimizing annealing time, which also includes heating (8°/K) and rapid cooling by switching off the heating with $ZnCl_2$ remaining in a molten state for about 15 min. The second sample was annealed at 853 K for 3 h, which is sufficient for a nearly complete transformation of the MAX phase sample into MXene, according to the in situ data shown in Figure 1. Both samples were washed with water to remove excess $ZnCl_2$, and XRD patterns were recorded at ambient temperature on air (Figure 4).

The sample prepared by annealing Ti_3AlC_2 in a molten $ZnCl_2$ for a longer time (3 h) shows strong reflections from MXene $Ti_3C_2Cl_x$ and reflections from metallic zinc, both in good agreement with literature data (Figure 4).[20] The sample annealed in molten $ZnCl_2$ for a short time (1 min at a maximal temperature of 853 K) showed only traces of (002) reflections from both the MAX phase and MXene. However, the sample shows several broader reflections, suggestively belonging to Ti_3C_2 layers, and relatively strong reflections identified as metallic Zn.

The data shown in Figure 4 suggest that the drop in the intensity of major XRD reflections of the MAX phase observed in situ at the initial stage of annealing (Figure 1) is due to a true disruption of the material's structure and nearly complete

https://doi.org/10.1021/acs.chemmater.4c02989
Chem. Mater. 2025, 37, 1132−1142

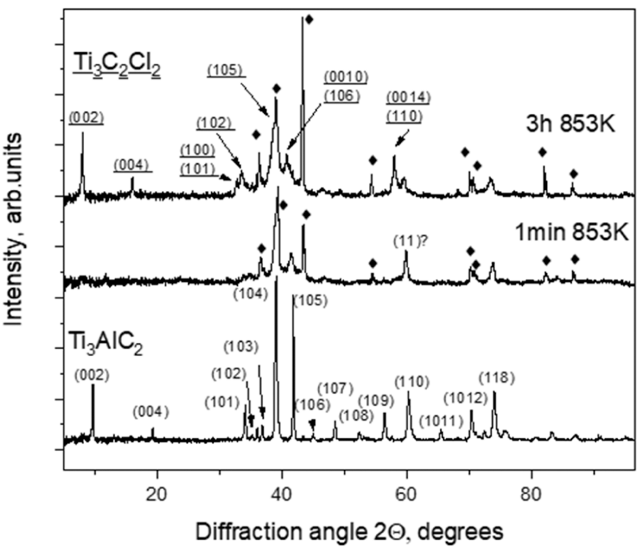

Figure 4. XRD patterns recorded using a conventional diffractometer (Cu Kα radiation) from a bulk sample of Ti_3AlC_2 and two samples of $Ti_3AlC_2/ZnCl_2$ mixture (1:6 molar) heated rapidly up to 853 K and annealed for 1 min and 3 h. The heating time with a rate of 8 °C/min adds about 30 min of exposure of the MAX phase to $ZnCl_2$ melt, and as fast as possible cooling of the furnace adds about 15 min required for melt to solidify. The samples were rapidly cooled back to ambient temperature to quench the high-temperature phases. Reflections due to metallic Zn are marked by (♦) symbols.

disorder of the 2D layers packing rather than the effect of bubble formation and turbulence inside the capillary.

Moreover, ex situ data suggest that metallic zinc is formed in these samples only after dissolving the excess of $ZnCl_2$ by washing with water. Metallic Zn was not found in our in situ experiments during both annealing and crystallization of the salt due to cooling. Therefore, most of the Zn formed as a reaction product between Al and $ZnCl_2$ should be dissolved in the molten salt. The relatively high intensity of Zn reflections indicates that the etching reactions proceeded rather rapidly. About 10−20 min of annealing with only 1 min at the maximum temperature of 853 K was sufficient for etching away most of the Al (removed as $AlCl_3$ gas) while Zn dissolved in the $ZnCl_2$ melt.

Analyses of XRD data recorded in situ (Figure 3) and ex situ (Figure 4) indicate that delaminated 2D sheets can be considered as intermediate states between the MAX phase and MXene. Most of the Al is likely to be already removed from the MAX phase and most of the Zn is dissolved in the molten salt in the delaminated state. XRD data also indicate that the "delaminated phase" is only partly converted into MXene after 3 h of annealing. The XRD pattern shown in Figure 3 is likely to include some reflections from the delaminated phase not restacked into the ordered MAX phase, as indicated, e.g., by a broader and stronger (105) reflection than expected (see Figure S6, where the experimental XRD pattern and simulated pattern of $Ti_3C_2Cl_2$ are compared).

In situ experiments presented here provide insights into the mechanism of MXene synthesis by the LAMS method (see the Discussion section). It should be mentioned with caution for future experiments that some additional reaction products were found in two less successful experiments due to the partial reaction of materials with water released from easily hydrated $ZnCl_2$ inside the capillary. Water is very easily absorbed by $ZnCl_2$ even after a short exposure to air. This water is released after heating due to the thermal decomposition of the hydrates, and then it moves and condenses in a cold zone of capillary prior to the melting of salt. However, when a larger diameter heating gun (and a smaller cold zone) was used, for the samples premixed in proportions of 1:6 and 1:9, experiments showed incomplete transformation of the MAX phase into MXene and the appearance of additional undesirable reaction products. The new "parasitic" phase appeared in these experiments shortly (15 min) after the melting of $ZnCl_2$ with the strongest characteristic reflections at 8.372, 3.377, and 2.765 Å (Figure S8). These reflections were indexed as (001), (101), and (011) of TiOCl. Using five strong reflections, the unit cell parameters of this phase were calculated as a = 3.688 Å, b = 3.381 Å, and c = 8.368 Å ($Pmmn$), which are slightly higher than ambient temperature values of TiOCl[37] due to thermal expansion of the material. It is known that TiOCl can be formed by the reaction of titanium oxide with titanium chloride at temperatures close to our experiments.[38] Formation of TiOCl was not observed in experiments with a larger heating gun only for the sample with a smaller $ZnCl_2$ loading (1:3) (Figure S9), confirming that the formation of TiOCl is related to water included in partly hydrated $ZnCl_2$. However, only a relatively small part of the MAX phase was converted to MXene in this experiment due to an insufficient amount of molten $ZnCl_2$. Notably, the same structure of MXene was found even in the experiments where the additional TiOCl phase was formed.

It can be concluded that using water-free salts and a sufficiently large "cold zone" for the condensation of reaction products is an important condition for the complete conversion of the MAX phase into MXene in sealed capillaries. Incomplete conversion of the MAX phase into MXene and the appearance of undesirable side products can be avoided.

In Situ Study of the MAX Phase Reaction with $SnCl_2$. The reaction of the MAX phase with molten $SnCl_2$ was studied in situ by XRD using the same procedure as in experiments with molten $ZnCl_2$ described above. Samples were mixed in molar ratios 1:3, 1:6, and 1:9 (MAX phase/$SnCl_2$) and annealed at 853−873 K for 6 h.

Similar to experiments with $ZnCl_2$, vigorous evolution of gas bubbles ($AlCl_3$) was observed in the initial stages of the reaction, and at the same time, the color of the sample changed from black to brown (see Figure S11 and Video in the SI). However, complete transformation was not achieved within 6 h in experiments with etching the MAX phase with molten SnO_2, even in the experiment with the highest salt loading molar ratio (1:9) and a temperature of 873 K (Figure 5).

Experiments with a smaller amount of loaded $SnCl_2$ and a lower temperature of 853 K showed also slower kinetics of the reaction and less complete conversion of Ti_3AlC_2 into MXene. This result is in agreement with an earlier ex situ study of MAX phase etching with $SnCl_2$ where incomplete conversion was observed after annealing for 8 h at 873 K.[21] However, unlike ex situ results,[21] no metallic Sn was detected in our XRD experiments (similar to the absence of Zn in experiments with $ZnCl_2$) even after cooling and solidification of the melt, suggesting that Sn dissolves in molten $SnCl_2$. The detailed analysis of XRD data is complicated by significant overlap of reflections from MXene, the remaining MAX phase, and the TiC phase. Nevertheless, the unit cell parameters of MXene $Ti_3C_2Cl_x$ produced by the etching of the MAX phase with $SnCl_2$ for the pattern recorded at the end of annealing at 873 K

https://doi.org/10.1021/acs.chemmater.4c02989
Chem. Mater. 2025, 37, 1132−1142

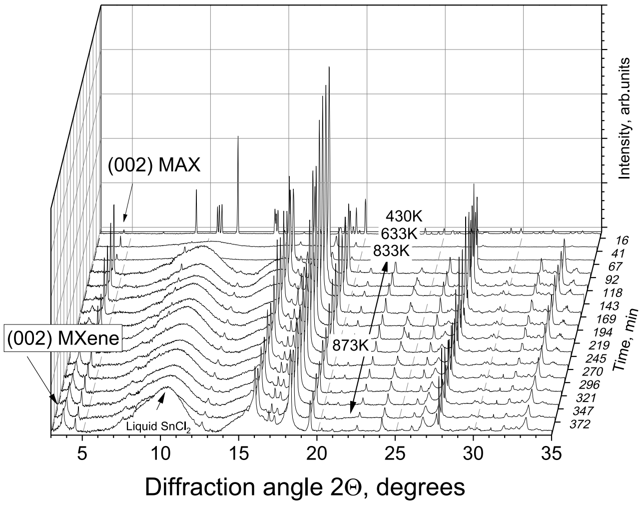

Figure 5. Selected XRD patterns (λ = 0.73804 Å) recorded during the in situ experiment with MAX phase etching by molten $SnCl_2$. The MAX phase and $SnCl_2$ were mixed in a 1:9 proportion (molar ratio) and annealed at 873 K.

(a = 3.18 Å and c = 22.287 Å, $P6_3/mmc$) appeared to be in remarkably good agreement with the experiments involving $ZnCl_2$ etching.

Similar to the experiments with $ZnCl_2$, annealing of the MAX phase in molten $SnCl_2$ goes through the stage of intense bubbling correlated with loss of ordering of Ti_3C_2 layers (Figure 5), suggesting the formation of a delaminated phase intermediate between the MAX phase and MXene. The MXene phase starts to emerge after about 1 h of annealing at 873 K (Figure 6b). Formation of other intermediate phases was not observed, similar to the experiment with $ZnCl_2$.

The reaction can be followed by the change in the relative intensity of (002) reflections of the MAX phase and MXene over the whole period of annealing (Figure 6c). The d(002) values of the MAX phase and MXene remain almost unchanged during annealing. Small shifts observed during heating are due to thermal expansion, as evidenced by the reverse change recorded during cooling (Figure 6a,b). The relative integral intensity of MXene(002)/MAX(002) reflections showed an approximately linear increase during annealing at 873 K (Figure 6c). It is obvious that the conversion of the MAX phase into MXene still continues after 6 h of annealing at 873 K (Figure 6c).

Extrapolating the time dependence shown in Figure 6c, it can be suggested that complete conversion of the MAX phase into MXene could possibly be achieved after prolonged (12–18 h) annealing. The slow kinetics and limitations of synchrotron time available for long experiments prevented us from obtaining pure MXene in this experiment.

Summarizing this part, experiments with the MAX phase in molten $SnCl_2$ showed very similar results to the ones in $ZnCl_2$. The same MXene phase was formed by etching the MAX phase with $ZnCl_2$ and $SnCl_2$ but the kinetics of the reaction was slower. Experiments with Ti_3AlC_2 etched with $SnCl_2$ reveal the same mechanism of the MXene formation from the MAX phase, which includes loss of ordering of Ti_3C_2 layers and formation of the "delaminated" phase as an intermediate product. Restacking of the chlorine-terminated 2D layers of the delaminated phase into $Ti_3C_2Cl_x$ MXene occurs during longer

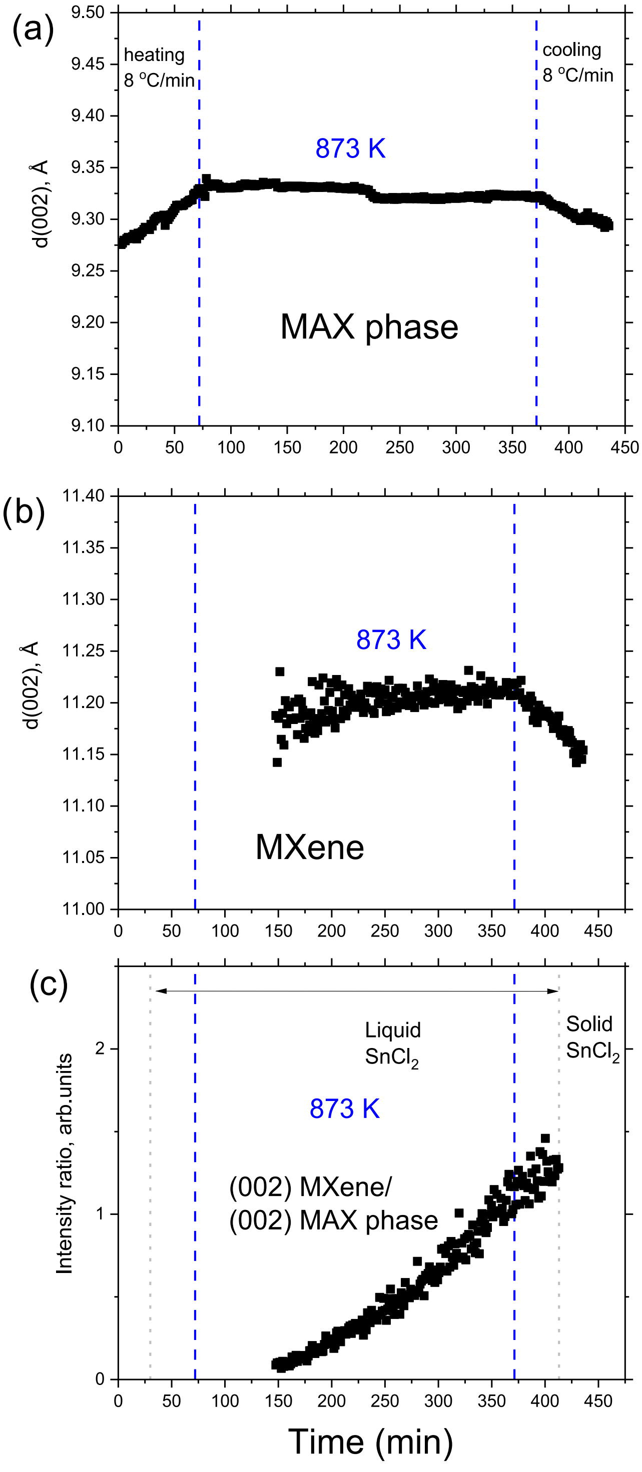

Figure 6. Evolution of (002) reflections from the MAX phase and MXene over the heating–cooling experiment in molten $SnCl_2$ (selected XRD patterns shown in Figure 5). The experiment includes heating up to 873 K, annealing at this temperature, and cooling back to ambient temperature.

annealing. The $Ti_3C_2Cl_x$ phase shows no swelling in molten $SnCl_2$ and remains unchanged after cooling and water washing.

DISCUSSION

The experiments presented above provide a detailed time-resolved characterization of structural transformations between the precursor MAX phase and MXene evaluated in situ directly

https://doi.org/10.1021/acs.chemmater.4c02989
Chem. Mater. 2025, 37, 1132−1142

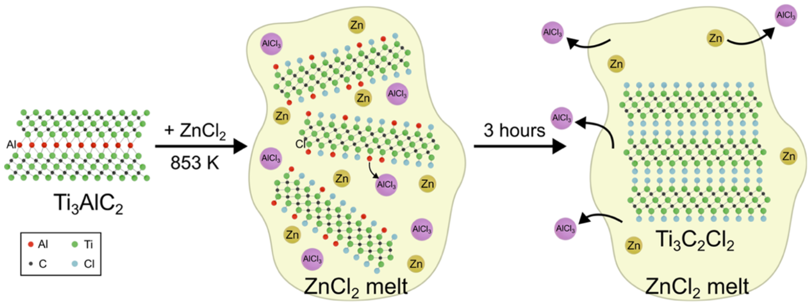

Figure 7. Schematic diagram illustrating the mechanism of the Ti_3AlC_2 reaction with molten ZnC_2 and formation of chlorine-terminated $Ti_3C_2Cl_x$ MXene.

in molten $ZnCl_2$ and $SnCl_2$. The data allow us to confirm the main points previously reported in ex situ studies[20,22,25,35] and provide insights into the mechanism of MAX phase etching in molten salts.

The main experimental observations reported above can be summarized as follows.

- The disordered delaminated phase is found during the first stage of Ti_3AlC_2 annealing (∼10−20 min) in both $ZnCl_2$ and $SnCl_2$. This phase can be considered an intermediate between Ti_3AlC_2 and MXene with 2D layers in a disordered state. This observation is in agreement with the only previously published in situ study of Nb_2GaC etching in molten salts, which reported complete amorphization of their materials at the initial stages of etching with the MXene structure emerging after prolonged annealing.[30]
- Rapid formation of gaseous $AlCl_3$ visually observed inside the capillary at the initial stage of the reaction is accompanied by the dissolution of Zn in molten $ZnCl_2$. Crystallization of metallic Zn occurs only when the salt is dissolved by water after cooling and melt solidification.
- The delaminated Ti_3C_2 layers are terminated by chlorine and restacked into the MXene structure. The first reflections of MXene appeared after ∼15−20 min of annealing at 853 K (for $ZnCl_2$), and the reaction is mostly completed after ∼3 h.
- No swelling of $Ti_3C_2Cl_x$ was found in both molten $ZnCl_2$ and $SnCl_2$. Molten salts cannot penetrate between Cl-terminated Ti_3C_2 layers. The MXene structure found directly in molten salts is the same as the one observed after cooling and water washing at ambient temperature (except for the effects of thermal expansion).
- Crystallization (restacking) of $Ti_3C_2Cl_x$ in the molten $ZnCl_2$ explains the better ordering of the MXene structure as compared to MXenes produced using solution-based methods.
- No other crystalline intermediate phases were observed in our in situ experiments. Experimental data revealed only reflections of Ti_3AlC_2, TiC, and MXene.
- Annealing in both $ZnCl_2$ and $SnCl_2$ showed qualitatively very similar reaction pathways providing the same Cl-terminated MXene phase in the end, in agreement with ex situ studies performed using a variety of etching salts.[18,20,24,25,27,39]

These results provide insights into the mechanism of MAX phase-to-MXene conversion by annealing in molten salt.

According to the mechanism of MXene synthesis proposed in earlier studies, Al is etched away from Ti_3AlC_2 by the reaction with molten salt and evaporates as $AlCl_3$ gas with simultaneous termination of titanium carbide layers by chlorine and formation of elemental zinc.[20,26] The synthesis of MXene is described by the following reactions.[26]

$$2Ti_3AlC_2(s) + 3ZnCl_2(liq) \rightarrow 2Ti_3C_2(s) + 2AlCl_3(g) + 3Zn(s) \quad (1)$$

$$2Ti_3C_2(s) + 2ZnCl_2(liq) \rightarrow 2Ti_3C_2Cl_2(s) + 2Zn(s) \quad (2)$$

In situ experiments presented in our study confirm these reactions but add significant insights to the mechanism of etching illustrated in Figure 7. The removal of Al from the MAX phase structure is found to be assisted by delamination of the Ti_3AlC_2 structure at step (1) of the reaction, evidenced by almost complete amorphization of the material. Delamination suggestively helps to expose all surfaces of 2D sheets to the $ZnCl_2$ melt, which makes reaction step (2) possible.

The delamination is likely to occur due to formation and rapid escape of gaseous $AlCl_3$, "exploding" the MAX phase structure. Therefore, the high vapor pressure of $AlCl_3$ formed much above its boiling point (453 K) at 850 K is likely to assist in the delamination of the MAX phase structure. In principle, the delamination can also be considered as extreme swelling of the material in the molten salt.

Analysis of our data suggests that once delaminated, the Ti_3C_2 sheets get rapidly terminated by chlorine, while Al escapes in the form of gaseous $AlCl_3$, and elemental Zn (or Sn) is dissolved in the molten salt.[40] Note that metallic zinc was not found in our experiments, even after cooling and salt solidification. Most likely, the absence of metallic Zn prior to water washing is explained by the previously reported formation of a Zn-enriched glass phase after rapid cooling of the $ZnCl_2$ melt with dissolved Zn.[20,40] Removing Al from the MAX phase interlayers with simultaneous termination of Ti_3C_2 layers with chlorine seems to be in agreement with in situ data collected in our study.

The MXene structure is found to appear after ∼20 min of annealing of the disordered delaminated phase and is suggestively formed by the restacking of Cl-terminated Ti_3C_2 flakes. The molten salt is expelled from the structure of MXene during the restacking, as evidenced by the absence of swelling.

The absence of the melt-swollen MXene phase is a nontrivial result considering that the XRD was recorded in our experiments from the MXene immersed in liquid molten $ZnCl_2$ (or $SnCl_2$). That is in strong contrast to our recent in situ studies of solution synthesis, which demonstrated the

https://doi.org/10.1021/acs.chemmater.4c02989
Chem. Mater. 2025, 37, 1132−1142

existence of the MXene structure with the c-lattice expanded by ~3 Å due to swelling in LiCl + HF solution (essentially in HF acid).[17] Thanks to swelling, HF solutions are capable of penetrating into interlayers of MXene. The etching reaction then proceeds by slow conversion of the MAX phase with MXene propagating along the interlayers with both phases coexisting for prolonged periods of time.[17]

The swelling of MXene in water is related to −OH termination of Ti_3C_2 layers.[13,31,41] Therefore, swelling of Cl-terminated MXene in molten chloride salts could also be expected following the general "like dissolves like" principle.

The absence of MXene swelling in molten $ZnCl_2$ and $SnCl_2$ indicates a different mechanism of the MAX phase etching reaction rather than slow etching along narrow interlayers. The MXene phase appears in our experiments only after nearly complete amorphization of the MAX phase, which is suggestively related to delamination of Ti_3C_2 layers.

The molten salt is not capable of penetrating between Cl-terminated layers of MXene, thus excluding the possibility of slow etching starting from the entrance points of interlayers and propagating slowly toward the inner parts. In the absence of MXene swelling in molten salts, formation of the delaminated phase is the only way to provide salt access to the whole surface of Ti_3C_2.

The reaction diagram shown in Figure 7 does not include the TiC side product, which is very commonly found in LAMS synthesis.[20] This phase is also evident in the in situ experiments presented here (Figure 3a). No other intermediate phases were found in our experiments.

Some earlier studies assumed the Zn-substituted phase as the "intermediate" phase in the reaction, leading to MXene formation.[19] However, formation of Zn-substituted MAX phase Ti_3ZnC_2 was reported only for experiments with a much smaller loading of $ZnCl_2$ (1:1.5 molar ratio).[25] Our experiments show no evidence for the presence of crystalline Zn- and Sn-substituted MAX phases in the reaction of Ti_3AlC_2 with molten salts loaded in larger amounts (1:6 and 1:9 molar ratios). A large excess of molten salt is expected to assist the reaction by more complete delamination of the MAX phase and by dissolution of Zn.[20] However, we cannot completely rule out the possible presence of the Zn-substituted phase if it is present in an amorphous state.

The Al substitution by Zn with the formation of crystalline Ti_3ZnC_2 seems to be unlikely due to Zn solubility in molten $ZnCl_2$. Dissolving Zn from the interlayers of the crystalline Ti_3ZnC_2 phase would require expansion of the c-lattice (swelling) to allow penetration of liquid salt inside the lattice interlayers. However, experimental data demonstrate that the absence of swelling and Ti_3ZnC_2 would be stable in a molten salt. Therefore, Zn- or Sn-substituted MAX phases can be considered as a side product (similar to TiC) rather than an intermediate phase.[19] The absence of intermediate Al-substituted MAX phases is in agreement with earlier ex situ studies, which reported that formation of Zn-substituted MXene is unfavorable in experiments with a larger excess of molten $ZnCl_2$.[20]

CONCLUSIONS

A time-resolved in situ study of MXene formation by MAX phase etching in molten salts was performed here using synchrotron radiation XRD. The main conclusions of the study are the following.

- The structure of MXenes formed by etching of the MAX phase with $ZnCl_2$ and $SnCl_2$ shows no swelling in molten salts. The MXene $Ti_3C_2Cl_x$ structure found in situ in the molten salt (a = 3.186 Å and c = 22.312 Å, $P6_3/mmc$) and after cooling and salt solidification is the same except for the effects of thermal expansion.
- The absence of $Ti_3C_2Cl_x$ swelling in molten salts is a nontrivial result. It shows that molten salts are expelled from the structure at the moment of MXene formation and are not capable of penetrating between chlorine-terminated Ti_3C_2 layers.
- That is in strong contrast to synthesis in aqueous solutions, where pristine MXene with a structure swollen in HF solution is formed during Al etching.[17] In the absence of swelling, the formation of MXene is not possible by gradual removal of Al from MAX phase interlayers starting at the edges of flakes and propagating into the deeper parts of interlayers.
- MXene formation occurs through an intermediate disordered delaminated phase formed at the initial stage of annealing in the molten salt.
- The termination of Ti_3C_2 layers by chlorine suggestively occurs in the disordered delaminated phase simultaneously with $AlCl_3$ formation and Zn dissolution in the molten salt. No other intermediate phases were found.
- The crystalline ordered MXene structure suggestively forms in the molten salt by restacking of 2D $Ti_3C_2Cl_x$ layers present in the delaminated disordered intermediate state.
- The in situ data suggest that Zn is dissolved in molten $ZnCl_2$. Metallic Zn (or other metals) typically found in ex situ studies[20,24] is not found prior to water washing.

In the future, it will be interesting to expand the in situ XRD experiments conducted in this study for molten salt etching of Ti_3AlC_2 to include other MAX phases and MXenes. Moreover, in situ studies of several other MXene synthesis procedures could contribute to the understanding of similarities and differences in the mechanism of MAX phase etching.

ASSOCIATED CONTENT

Supporting Information

The Supporting Information is available free of charge at https://pubs.acs.org/doi/10.1021/acs.chemmater.4c02989.

Additional data and figures including indexing of the experimental Ti_3AlC_2 precursor; comparing the structure of the MAX phase prior to and after melting of $ZnCl_2$ at temperatures up to 853 K; experimental XRD patterns of the MAX phase and MXene compared to theoretically simulated patterns for Ti_3AlC_2, Ti_3ZnC_2, and $Ti_3C_2Cl_2$; additional data recorded in experiments with $SnCl_2$ etching; scanning electron microscopy (SEM) images of MXene samples; and optical images (PDF)

Video showing bubbles evolving inside of the sealed capillary at the initial stages of the etching reaction (MP4)

AUTHOR INFORMATION

Corresponding Author

Alexandr V. Talyzin − *Department of Physics, Umeå University, Umeå SE-901 87, Sweden;* orcid.org/0000-0002-3320-8487; Email: alexandr.talyzin@umu.se

https://doi.org/10.1021/acs.chemmater.4c02989
Chem. Mater. 2025, 37, 1132−1142

Authors

Artem Iakunkov − *School of Engineering Sciences in Chemistry, Biotechnology and Health, KTH Royal Institute of Technology, Stockholm SE-100 44, Sweden*

Nicolas Boulanger − *Department of Physics, Umeå University, Umeå SE-901 87, Sweden*

Bartosz Gurzeda − *Department of Physics, Umeå University, Umeå SE-901 87, Sweden*

Gui Li − *Department of Physics, Umeå University, Umeå SE-901 87, Sweden*

Christoph Hennig − *Institute of Resource Ecology, Helmholtz Zentrum Dresden Rossendorf, 01328 Dresden, Germany; The Rossendorf Beamline, European Synchrotron Radiation Facility, Grenoble 38043, France;* orcid.org/0000-0001-6393-2778

Volodymyr Svitlyk − *Institute of Resource Ecology, Helmholtz Zentrum Dresden Rossendorf, 01328 Dresden, Germany; The Rossendorf Beamline, European Synchrotron Radiation Facility, Grenoble 38043, France;* orcid.org/0000-0001-5449-8009

Mads Ry Vogel Jørgensen − *Department of Chemistry and INANO, Aarhus University, DK-8000 Aarhus C, Denmark; MAX IV Laboratory, Lund University, Lund 22594, Sweden;* orcid.org/0000-0001-5507-9615

Innokenty Kantor − *Department of Chemistry and INANO, Aarhus University, DK-8000 Aarhus C, Denmark*

Igor A. Baburin − *Earth and Environmental Sciences, Ludwig-Maximilians-Universität München, 80333 München, Germany*

Mahiar Max Hamedi − *School of Engineering Sciences in Chemistry, Biotechnology and Health and Wallenberg Initiative Materials Science for Sustainability, KTH Royal Institute of Technology, Stockholm SE-100 44, Sweden;* orcid.org/0000-0001-9088-1064

Complete contact information is available at:
https://pubs.acs.org/10.1021/acs.chemmater.4c02989

Notes

The authors declare no competing financial interest.

■ ACKNOWLEDGMENTS

Energimyndigheten (grant number No. 50620-1) is acknowledged for financial support Kempestiftelserna are acknowledged for stipend funding to employ B.G. The authors acknowledge the ESRF and CRG support for providing synchrotron radiation beam time (experiment number: A20-1-860) on the BM20 (ROBL) beamline. The authors acknowledge MAX IV Laboratory for time on Beamline DanMAX under Proposal 20221405. Research conducted at MAX IV is supported by the Swedish Research Council under contract 2018-07152, the Swedish Governmental Agency for Innovation Systems under contract 2018-04969, and Formas under contract 2019-02496. DanMAX is funded by the NUFI grant no. 4059-00009B. A.I. and M.M.H. acknowledge the Swedish Energy Agency (Energimyndigheten) for funding this project (grant number 48489-1).

■ REFERENCES

(1) Gogotsi, Y.; Anasori, B. The Rise of MXenes. *ACS Nano* **2019**, *13* (8), 8491−8494.

(2) Mohammadi, A. V.; Rosen, J.; Gogotsi, Y. The world of two-dimensional carbides and nitrides (MXenes). *Science* **2021**, *372* (6547), 1165−1179.

(3) Pang, J.; Mendes, R. G.; Bachmatiuk, A.; Zhao, L.; Ta, H. Q.; Gemming, T.; Liu, H.; Liu, Z.; Rummeli, M. H. Applications of 2D MXenes in energy conversion and storage systems. *Chem. Soc. Rev.* **2019**, *48* (1), 72−133.

(4) Anasori, B.; Lukatskaya, M. R.; Gogotsi, Y. 2D metal carbides and nitrides (MXenes) for energy storage. *Nat. Rev. Mater.* **2017**, *2* (2), No. 16098, DOI: 10.1038/natrevmats.2016.98.

(5) Zhan, X.; Si, C.; Zhou, J.; Sun, Z. MXene and MXene-based composites: synthesis, properties and environment-related applications. *Nanoscale Horiz.* **2020**, *5* (2), 235−258.

(6) Hantanasirisakul, K.; Gogotsi, Y. Electronic and Optical Properties of 2D Transition Metal Carbides and Nitrides (MXenes). *Adv. Mater.* **2018**, *30* (52), No. 1804779.

(7) Huang, K.; Li, Z.; Lin, J.; Han, G.; Huang, P. Two-dimensional transition metal carbides and nitrides (MXenes) for biomedical applications. *Chem. Soc. Rev.* **2018**, *47* (14), 5109−5124.

(8) Rosenkranz, A.; Marian, M. Combining surface textures and MXene coatings—towards enhanced wear-resistance and durability. *Surf. Topogr.: Metrol. Prop.* **2022**, *10* (3), No. 033001.

(9) Melianas, A.; Kang, M.-A.; VahidMohammadi, A.; Quill, T. J.; Tian, W.; Gogotsi, Y.; Salleo, A.; Hamedi, M. M. High-Speed Ionic Synaptic Memory Based on 2D Titanium Carbide MXene. *Adv. Funct. Mater.* **2022**, *32* (12), No. 2109970.

(10) Naguib, M.; Kurtoglu, M.; Presser, V.; Lu, J.; Niu, J. J.; Heon, M.; Hultman, L.; Gogotsi, Y.; Barsoum, M. W. Two-Dimensional Nanocrystals Produced by Exfoliation of Ti3AlC2. *Adv. Mater.* **2011**, *23* (37), 4248−4253.

(11) Lukatskaya, M. R.; Mashtalir, O.; Ren, C. E.; Dall'Agnese, Y.; Rozier, P.; Taberna, P. L.; Naguib, M.; Simon, P.; Barsoum, M. W.; Gogotsi, Y. Cation Intercalation and High Volumetric Capacitance of Two-Dimensional Titanium Carbide. *Science* **2013**, *341* (6153), 1502−1505.

(12) Mashtalir, O.; Naguib, M.; Mochalin, V. N.; Dall'Agnese, Y.; Heon, M.; Barsoum, M. W.; Gogotsi, Y. Intercalation and delamination of layered carbides and carbonitrides. *Nat. Commun.* **2013**, *4*, No. 1716.

(13) Ghidiu, M.; Halim, J.; Kota, S.; Bish, D.; Gogotsi, Y.; Barsoum, M. W. Ion-Exchange and Cation Solvation Reactions in Ti3C2MXene. *Chem. Mater.* **2016**, *28* (10), 3507−3514.

(14) Alhabeb, M.; Maleski, K.; Anasori, B.; Lelyukh, P.; Clark, L.; Sin, S.; Gogotsi, Y. Guidelines for Synthesis and Processing of Two-Dimensional Titanium Carbide (Ti3C2Tx MXene). *Chem. Mater.* **2017**, *29* (18), 7633−7644.

(15) Ghidiu, M.; Kota, S.; Drozd, V.; Barsoum, M. W. Pressure-induced shear and interlayer expansion in Ti3C2MXene in the presence of water. *Sci. Adv.* **2018**, *4* (1), No. eaao6850.

(16) Zhang, T.; Pan, L.; Tang, H.; Du, F.; Guo, Y.; Qiu, T.; Yang, J. Synthesis of two-dimensional Ti3C2Tx MXene using HCl+LiF etchant: Enhanced exfoliation and delamination. *J. Alloys Compd.* **2017**, *695*, 818−826.

(17) Gurzęda, B.; Boulanger, N.; Nordenström, A.; Dejoie, K.; Talyzin, A. V. Pristine MXene: in situ XRD study of MAX phase etching with HCl+LiF solution. *Adv. Sci.* **2024**, *11*, No. 2408448.

(18) Ding, H.; Li, Y.; Li, M.; Chen, K.; Liang, K.; Chen, G.; Lu, J.; Palisaitis, J.; Persson, P. O. Å.; Eklund, P.; Hultman, L.; Du, S.; Chai, Z.; Gogotsi, Y.; Huang, Q. Chemical scissor−mediated structural editing of layered transition metal carbides. *Science* **2023**, *379* (6637), 1130−1135.

(19) Kruger, D. D.; García, H.; Primo, A. Molten Salt Derived MXenes: Synthesis and Applications. *Adv. Sci.* **2024**, No. 11, No. 2307106.

(20) Li, M.; Lu, J.; Luo, K.; Li, Y. B.; Chang, K. K.; Chen, K.; Zhou, J.; Rosen, J.; Hultman, L.; Eklund, P.; Persson, P. O. A.; Du, S. Y.; Chai, Z. F.; Huang, Z. R.; Huang, Q. Element Replacement Approach by Reaction with Lewis Acidic Molten Salts to Synthesize Nanolaminated MAX Phases and MXenes. *J. Am. Chem. Soc.* **2019**, *141* (11), 4730−4737.

(21) Wu, Z. Y.; Zhu, S.; Bai, X. R.; Liang, M.; Zhang, X.; Zhao, N. Q.; He, C. N. One-step in-situ synthesis of Sn-nanoconfined Ti3C2Tx

MXene composites for Li-ion battery anode. *Electrochim. Acta* **2022**, *407*, No. 139916, DOI: 10.1016/j.electacta.2022.139916.
(22) Khan, U.; Luo, Y. J.; Kong, L. B.; Que, W. X. Synthesis of fluorine free MXene through lewis acidic etching for application as electrode of proton supercapacitors. *J. Alloys Compd.* **2022**, *926*, No. 166903, DOI: 10.1016/j.jallcom.2022.166903.
(23) Bai, Y.; Liu, C. L.; Chen, T. T.; Li, W. T.; Zheng, S. S.; Pi, Y. C.; Luo, Y. S.; Pang, H. MXene-Copper/Cobalt Hybrids via Lewis Acidic Molten Salts Etching for High Performance Symmetric Supercapacitors. *Angew. Chem., Int. Ed.* **2021**, *60* (48), 25318−25322.
(24) Li, Y. B.; Shao, H.; Lin, Z. F.; Lu, J.; Liu, L. Y.; Duployer, B.; Persson, P. O. Å.; Eklund, P.; Hultman, L.; Li, M.; Chen, K.; Zha, X. H.; Du, S. Y.; Rozier, P.; Chai, Z. F.; Raymundo-Piñero, E.; Taberna, P. L.; Simon, P.; Huang, Q. A general Lewis acidic etching route for preparing MXenes with enhanced electrochemical performance in non-aqueous electrolyte. *Nat. Mater.* **2021**, *20* (4), 571.
(25) Lu, J.; Persson, I.; Lind, H.; Palisaitis, J.; Li, M.; Li, Y.; Chen, K.; Zhou, J.; Du, S.; Chai, Z.; Huang, Z.; Hultman, L.; Eklund, P.; Rosen, J.; Huang, Q.; Persson, P. O. Å. Tin+1Cn MXenes with fully saturated and thermally stable Cl terminations. *Nanoscale Adv.* **2019**, *1* (9), 3680−3685.
(26) Zhang, T.; Shevchuk, K.; Wang, R. J.; Kim, H.; Hourani, J.; Gogotsi, Y. Delamination of Chlorine-Terminated MXene Produced Using Molten Salt Etching. *Chem. Mater.* **2024**, *36* (4), 1998−2006.
(27) Liu, L. Y.; Orbay, M.; Luo, S.; Duluard, S.; Shao, H.; Harmel, J.; Rozier, P.; Taberna, P. L.; Simon, P. Exfoliation and Delamination of Ti3C2Tx MXene Prepared Molten Salt Etching Route. *ACS Nano* **2022**, *16* (1), 111−118.
(28) Wang, F.; Tian, F.; Xia, X. W.; Pang, Z. Y.; Wang, S. J.; Yu, X.; Li, G. S.; Zhao, Y. F.; Xu, Q.; Hu, S.; Ji, L.; Zou, X. L.; Lu, X. G. One-step Synthesis of Organic Terminal 2D Ti3C2Tx MXene Nanosheets by Etching of Ti3AlC2 in an Organic Lewis Acid Solvent. *Angew. Chem., Int. Ed.* **2024**, *63* (23), No. e202405315, DOI: 10.1002/anie.202405315.
(29) Shen, M.; Jiang, W. Y.; Liang, K.; Zhao, S. F.; Tang, R.; Zhang, L. J.; Wang, J. Q. One-Pot Green Process to Synthesize MXene with Controllable Surface Terminations using Molten Salts. *Angew. Chem., Int. Ed.* **2021**, *60* (52), 27013−27018.
(30) Wei, S. Q.; Zhang, P. J.; Xu, W. J.; Chen, S. M.; Xia, Y. J.; Cao, Y. Y.; Zhu, K. F.; Cui, Q. L.; Wen, W.; Wu, C. Q.; Wang, C. D.; Song, L. Operando Exploring and Modulating Phase Evolution Chemistry from MAX to MXenes in Molten Salt Synthesis. *J. Am. Chem. Soc.* **2023**, *145* (19), 10681−10690.
(31) Célérier, S.; Hurand, S.; Garnero, C.; Morisset, S.; Benchakar, M.; Habrioux, A.; Chartier, P.; Mauchamp, V.; Findling, N.; Lanson, B.; Ferrage, E. Hydration of Ti3C2Tx MXene: An Interstratification Process with Major Implications on Physical Properties. *Chem. Mater.* **2019**, *31* (2), 454−461.
(32) Dyadkin, V.; Pattison, P.; Dmitriev, V.; Chernyshov, D. A new multipurpose diffractometer PILATUS@SNBL. *J. Synchrotron Radiat.* **2016**, *23* (3), 825−829.
(33) Kieffer, J.; Valls, V.; Blanc, N.; Hennig, C. New tools for calibrating diffraction setups. *J. Synchrotron Radiat.* **2020**, *27*, 558−566.
(34) Jensen, A. B.; Christensen, T. E. K.; Weninger, C.; Birkedal, H. Very large-scale diffraction investigations enabled by a matrix-multiplication facilitated radial and azimuthal integration algorithm: MatFRAIA. *J. Synchrotron Radiat.* **2022**, *29*, 1420−1428.
(35) Li, Y. B.; Shao, H.; Lin, Z. F.; Lu, J.; Liu, L. Y.; Duployer, B.; Persson, P. O. Å.; Eklund, P.; Hultman, L.; Li, M.; Chen, K.; Zha, X. H.; Du, S. Y.; Rozier, P.; Chai, Z. F.; Raymundo-Piñero, E.; Taberna, P. L.; Simon, P.; Huang, Q. A general Lewis acidic etching route for preparing MXenes with enhanced electrochemical performance in non-aqueous electrolyte. *Nat. Mater.* **2020**, *19* (8), 894−899.
(36) Iakunkov, A.; Nordenstrom, A.; Boulanger, N.; Hennig, C.; Baburin, I.; Talyzin, A. V. Temperature-dependent swelling transitions in MXene Ti3C2Tx. *Nanoscale* **2022**, *14* (30), 10940−10949.
(37) Schäfer, H.; Wartenpfuhl, F.; Weise, E. Uber Titanchloride. 5. Titan(Iii)-Oxychlorid. *Z. Anorg. Allg. Chem.* **1958**, *295* (3−4), 268−280.
(38) Sekimoto, H.; Nose, Y.; Uda, T.; Sugimura, H. Preparation and Properties of Trivalent Titanium Compounds, TiCl and TiOCl. *High Temp. Mater. Processes* **2011**, *30* (4−5), 435−440.
(39) Yan, M.; Zhu, Y.; Huang, J. T.; Chen, H. Y.; Deng, Y. X.; Chen, Y. L.; Wang, J.; Albina, J. M. Etching Mechanism of Ti3C2Cl2MXene Phases by CuCl2 -Lewis Molten Salt Method. *J. Wuhan Univ. Technol., Mater. Sci. Ed.* **2024**, *39* (4), 863−868.
(40) Kerridge, D. H.; Tariq, S. A. Solution of Zinc in Fused Zinc Chloride. *J. Chem. Soc. A* **1967**, No. 7, 1122−1125.
(41) Ghidiu, M.; Lukatskaya, M. R.; Zhao, M. Q.; Gogotsi, Y.; Barsoum, M. W. Conductive two-dimensional titanium carbide 'clay' with high volumetric capacitance. *Nature* **2014**, *516* (7529), 78−81.